NIH Public Access
Author Manuscript
Pain. Author manuscript; available in PMC 2013 January 1.

Published in final edited form as:
Pain. 2012 January ; 153(1): 158–169. doi:10.1016/j.pain.2011.10.006.

Differential fMRI Activation to Noxious Heat and Tactile Stimuli in Parasylvian Areas of New World Monkeys

Li Min Chen[1,2,*], **Barbara C Dillenburger**[1,2], **Feng Wang**[1,2], and **ChaoHui Tang**[1,2]

[1]Department of Radiology and Radiological Science, Vanderbilt University, Nashville, TN, USA

[2]Institute of Imaging Science, Vanderbilt University, Nashville, TN, USA

Abstract

Emerging evidence supports an important role of posterior parasylvian areas in both pain and touch processing. Whether there are separate or shared networks for these sensations remains controversial. The present study compared spatial patterns of brain activation in response to unilateral nociceptive heat (47.5° C) or innocuous tactile stimulation (8 Hz vibration) to digits through high-resolution fMRI in squirrel monkeys. In addition, the temporal profile of heat stimulus evoked fMRI BOLD signal changes was characterized. By examining high-resolution fMRI and histological measures at both the individual and group levels, we found that both nociceptive heat and tactile stimuli elicited activation in bilateral secondary somatosensory and ventral parietal areas (S2/PV) and in ipsilateral ventral somatosensory area (VS) and retroinsula (Ri). Bilateral posterior insular cortex (pIns) and area 7b responded preferentially to nociceptive heat stimulation. Single voxels within each activation cluster showed robust BOLD signal changes during each block of nociceptive stimulation. Across animals (n = 11), nociceptive response magnitudes of contralateral VS and pIns, and ipsilateral Ri were significantly greater than corresponding areas in the opposite hemisphere. In sum, both distinct and shared areas in regions surrounding the posterior sylvian fissure were activated in response to nociceptive and tactile inputs in non-human primates.

Keywords

nociception; hand; primates; cortex; touch; fMRI

Introduction

A growing body of evidence, particularly from functional imaging studies in humans, supports an essential role of the parasylvian region, including secondary somatosensory (SII) and insular cortices, in the processing of pain, touch, thermoreception (e.g. cold) and sense of internal homeostatis [1; 11; 12; 21; 22]. Numerous studies have found that various painful stimuli activate areas in the parasylvian region (for reviews see [1; 71; 88], lesions or

© 2011 International Association for the Study of Pain. Published by Elsevier B.V. All rights reserved.

*Corresponding author: Li Min Chen, M.D., Ph.D., AA 1105 MCN, 1161 21st Ave. S., Nashville, TN, 37027, USA, Tel: 1 615 9367069, Fax: 1 615 3220734, limin.chen@vanderbilt.edu.

Publisher's Disclaimer: This is a PDF file of an unedited manuscript that has been accepted for publication. As a service to our customers we are providing this early version of the manuscript. The manuscript will undergo copyediting, typesetting, and review of the resulting proof before it is published in its final citable form. Please note that during the production process errors may be discovered which could affect the content, and all legal disclaimers that apply to the journal pertain.

conflict of interest statement:
There is no financial conflict of interest in publishing this manuscript.

NIH-PA Author Manuscript
NIH-PA Author Manuscript
NIH-PA Author Manuscript

NIH-PA Author Manuscript

NIH-PA Author Manuscript

NIH-PA Author Manuscript

stimulation of this region alter pain sensitivity [4; 7; 42; 44; 64; 94] and electrical activities are recorded directly from this region in response to painful stimuli in humans [58; 76; 90; 95]. It has been postulated that the parasylvian region might be the earliest cortical pain specific processing region [47; 73; 74]. This region has been shown to be involved in the recognition of the nature of pain [60; 82; 85], pain intensity [66; 70; 72; 85], learning and memory of painful events [27] and the generation and maintenance of chronic pain states [1; 81]. Though the functional importance of the parasylvian region, particularly of the posterior portion, in pain perception has been well established, the precise nature of these functions and the underlying neuronal mechanisms remain unclear. Current evidence supports that the posterior portion of the parasylvian region, including the classical SII region (including subregions of S2/PV/VS) and posterior insula, is involved in the processing of painful and tactile information [3; 5; 11; 12; 26; 37–39; 42; 67; 77–79; 86; 91]. However, whether separate or shared cortical networks process touch and painful information remains controversial [34; 35; 59; 61; 84; 95]. The present study attempts to address this issue by directly comparing brain activation in response to nociceptive heat and innocuous tactile stimuli in areas along the sylvian fissure of individual anesthetized squirrel monkeys through high-resolution fMRI.

To date, there is limited knowledge of the response properties of paraslyvian nociceptive neurons and thus, understanding the role of the operculo-insular region in nociceptive processing and pain perception has been difficult [27; 28; 77]. A systematic evaluation of the functional organization and electrophysiological properties of nociceptive neurons within the parasylvian region is urgently needed. The present study employed an ultra-high (9.4T) MRI field for optimal spatial resolution in separating nociceptive and tactile responses within the anatomically and functionally complex parasylvian region. The power and success of this approach have been illustrated in various sensory systems in both human and monkey studies [3; 13; 17; 29; 30; 40; 41; 62; 63; 83]. As a first step toward a better understanding of the neuronal mechanisms underlying the sensory representation of pain, we applied submillimeter resolution fMRI in anesthetized squirrel monkeys at 9.4T to: 1) map and identify areas along the parasylvian region that are responsive to heat nociceptive stimuli, 2) compare spatially the nociceptive and innocuous tactile response patterns, and 3) characterize the temporal properties of nociceptive heat responsive areas. High resolution fMRI activation maps obtained in individual monkeys will provide the framework for future invasive electrophysiological studies.

Methods and Materials

Animal Preparation

fMRI scans were performed in eleven anesthetized squirrel monkeys while experiencing either a noxious heat stimulus (all subjects, one subject scanned twice) or an innocuous tactile stimulus (9 of the 11 subjects). Each animal was initially sedated with ketamine hydrochloride/atropine and then maintained on mechanical ventilation while isoflurane anesthesia (0.5–1.1%) was delivered in a 70:30 N_2O:O_2 mixture. Anesthetized animals were placed in a custom-designed MR cradle with heads immobilized. Lactated Ringer's solution containing 2.5% dextrose was infused intravenously (3ml/kg/hr) throughout the imaging session to prevent dehydration and to provide caloric energy. SpO_2 and heart rate (Nonin, Plymouth, MN), ECG, ET-CO_2 (22–26 mmHg; Surgivet, Waukesha, WI), and respiratory patterns (SA instruments, Stony Brook, NY) were continuously monitored. Rectal temperature was monitored (SA instruments) and maintained between 37.0 – 38.5° C. Vital signs were monitored throughout the procedure from induction of anesthesia until full recovery. All procedures were in compliance with and approved by the Institutional Animal Care and Use Committee of Vanderbilt University.

NIH-PA Author Manuscript

NIH-PA Author Manuscript

NIH-PA Author Manuscript

Stimulus Protocol

Nociceptive heat—Animal fingers were secured by gluing small pegs (firmly fixed in plasticine) to the fingernails, leaving the digit glabrous surface available for thermal stimulation. A 30 × 30 mm^2 CHEPS thermode (Medoc, ramp rate of 70 °C/s) was positioned over the glabrous skin of the distal and middle phalanges of digits 2 – 5. Baseline temperature (32° C) was alternated with nociceptive thermal stimuli (47.5 ° C) found to elicit strong burning pain sensation in human subjects in unpublished psychophysics observations. The MR scanner controlled the stimulus timing by sending trigger pulses to the Medoc PATHWAY system (Medoc LTD, Israel) to start each stimulus epoch during an imaging run. In each imaging run, nine stimulus blocks (epochs) consisting of 30 sec of a baseline temperature followed by 24 sec of nociceptive thermal stimulus were presented. Typically, multiple imaging runs (2 – 4) for each stimulus condition were performed within one imaging session.

Innocuous tactile stimulation—Tactile stimulation (8 Hz tapping with 2 mm in diameter size probe in 0.34 mm vertical displacement) was presented to a single distal finger pad in each animal to map cortical responses in lateral sulcus areas. Tactile stimulation was presented either alone or within the same imaging sessions as nociceptive heat. Tactile stimulation was presented in 30 sec on and off blocks with seven repeats within one imaging run.

fMRI data acquisition and analysis

All scans were performed on a 9.4T 21 cm bore Varian Inova MR system (Varian, Palo Alto, CA) using a 6 cm surface transmit-receiver coil centered over the midline of the brain. Scout sagittal images using a gradient-echo sequence were used to define the imaging volume, and to locate coronal slices for structural and functional images. After shimming over this volume, five 2-mm thick T2*-weighted gradient echo structural images (repetition time (TR), 200 ms; echo time (TE), 14 ms, 512 × 512 matrix; 78 × 78 × 2000 μm^3 resolution) were acquired to visualize gray and white matter contrast, and to identify brain structural features for coregistration of MRI maps obtained across imaging sessions conducted on different days on the same animal, and across animals (one example is shown in Figure 1A). Five coronal slices were positioned to cover the posterior two-thirds of the lateral sulcus region, where the classical SII, insular cortices, and thalamus reside. Coronal images were placed according to the stereotactic framework, in an effort to insure alignment with each animal's corresponding histological sections (Figure 1), and with MRI images acquired across animals. Functional MRI data were acquired from the same five slices by using a gradient echo planar imaging (GE-EPI) sequence (TE = 16 ms; 64 × 64 matrix; 0.7 × 0.7 × 2 mm^3 or 0.35 × 0.35 × 2 mm^3 resolution). A TR of 1.5 s was determined to match ventilation rate in order to minimize respiration-induced signal variations in BOLD signal time courses.

Reconstructed images were imported into Matlab (Mathworks, Natick, MA) for analysis. The functional echo planar imaging (EPI) images first underwent distortion correction with B0 maps obtained within each imaging session. The time course of the EPI data was then drift corrected using a linear model fitted to each time course and temporally smoothed with a low-pass filter with a cut-off frequency set at 0.25 Hz. No spatial smoothing was applied in order to preserve the highest resolution possible. Voxel-wise correlation analysis of the BOLD time course to a boxcar function (delayed by 2 image volumes (3 sec) to compensate for the hemodynamic lag) was performed, and functional activation maps were generated by identifying voxels with significant correlations at $p \leq 10^{-4}$ ($p \leq 0.05$ with Bonferroni multiple comparison correction) and with a minimal cluster size of 2 voxels for each run. At 9.4T, a single functional imaging run, which has 300 – 340 image volumes comprising 9

NIH-PA Author Manuscript

NIH-PA Author Manuscript

NIH-PA Author Manuscript

heat or 7 tactile epochs of stimulus/baseline blocks was sufficient to generate activation maps at a reasonable statistical significance threshold of $p \leq 10^{-4}$ as we have demonstrated before [102]. To improve the overall confidence level of detected activation at different locations, we typically performed multiple runs and then generated one average activation map within each imaging session for each animal. These average activation maps, which were thresholded at $p \leq 0.01$ (uncorrected), were used to generate cross-animal activation frequency map. Activation maps were interpolated to the native resolution of the structural images, and overlaid on high-resolution structural images for display. All activation maps shown in this paper were derived from comparison of a single condition with baseline (rest). The focus of the present study was to investigate activation in the areas along the Sylvian Fissure and therefore, other cortical and subcortical regions were masked out in the illustrations.

Quantification of BOLD activation map across animals

Reliability of activation was evaluated at both the individual and group levels. Within each subject, repeated activation in at least two runs was used as the criterion for determining a reliable activation. One average activation map was generated for group analysis. At the group level, the reliability of activation across animals was assessed in two ways: activation frequency and probability map.

Activation frequency—Activation frequency for each particular cortical area (e.g. area 7b, S2/PV) was calculated across animals based on the average-run activation maps obtained for each animal (see above). Identification of activation location was determined by 1) the animal's corresponding histological sections in a subset of animals (n = 7) (examples shown in Figures 1 and 2), and 2) published cytoarchitectonic maps for this species [8; 50] in animals whose histological sections were not available (n = 4). Activation frequency for each area is summarized in Table 1. Detailed reference maps at each coronal plane are displayed in Figure 3.

Probability map—By overlaying each individual activation map to a common template we generated a probability map. One of the eleven animals was designated at random as a common template. In contrast to activation frequency, which reveals individual subject differences in brain anatomy and activation locations, probability maps were generated for assessing the reliability of activation at particular physical locations. The probability map was generated with procedures similar to normalization maps (activation maps morphed to one common brain template) routinely used in human fMRI studies. Procedurally, high resolution and high contrast structural images obtained from different animals were first aligned to one set of template brain slices (e.g. coronal slices obtained from monkey #1) according to their anatomical features. After alignment, the frequency of activation at each location was calculated for each slice in Matlab by a custom-made script.

BOLD signal time course analysis

To characterize BOLD signal changes at different cortical locations and across hemispheres, a region of interest (ROI)-based time course analysis was conducted in each animal and then averaged across animals for each particular ROI. Stimulus-related BOLD signal change is a relative measure and is calculated by subtracting pre-stimulus BOLD magnitude from post-stimulus BOLD magnitude and then dividing by pre-stimulus BOLD magnitude. As compared to the defined pre-stimulus baseline BOLD signal, BOLD signals of voxels can significantly increase (termed positive BOLD signal change) or decrease (termed negative BOLD signal change) or fluctuate around baseline during the presentation of stimuli. In our study, we have observed statistically significant BOLD signal decreases (negative BOLD) during nociceptive stimulation. However, we excluded the report of negative BOLD

NIH-PA Author Manuscript

NIH-PA Author Manuscript

NIH-PA Author Manuscript

activation in the present paper in order to keep the topic focused. Specifically, in each animal, % BOLD signal changes for each ROI were extracted from the top three peak voxels (with the highest p or t values) and then were averaged across runs (one example shown in Figure 5). Differences between contralateral and ipsilateral ROI BOLD signal changes were examined using a bootstrap analysis (for a detailed description see [25; 93], a method that has been used in fMRI studies and has shown reliability in assessing statistical significance [2]. We first parameterized the magnitude (peak and undershot) and temporal characteristic (time to peak, TTP) of the BOLD signal by fitting the average time courses of contralateral and ipsilateral ROIs (e.g. S2/PV) with a two-gamma function (for model details see ref. [101]). We then employed bootstrap statistical analysis by comparing the fitting parameters of the initial average time course with the distribution of the fitting parameters of the randomly created 1000 datasets of all the raw BOLD time courses of both hemispheres to evaluate whether changes of parameters between contralateral and ipsilateral ROIs were significantly different (two-tailed t-test).

Identification of cortical areas through MRI image coregistration with tissue histology

Upon completion of functional experiments, brain tissue containing the fMRI image volume from 7 subjects was cropped in a stereotactic frame, and cut coronally (40 um thick). Brain sections were stained for cytochrome oxidase (CO), Nissl, and vesicle glutamate transporter 2 (VGluT2). Standard tissue staining protocols were followed, with details described in [49; 75; 98]. VGluT2 immunostain reveals thalamocortical terminations in layer 4. Cytoarchitectural features were examined across serial slices with multiple stains (CO, Nissl, and VGluT2) to determine the inter-areal borders; for detailed descriptions of different cortical area features see [8; 50; 96]. The factors that contribute to the accuracy of alignment and identification of cortical areas are outlined in the discussion. For illustration purposes, CO, Nissl, and VGluT2 stained brain sections exhibiting closely matching anatomical features are shown in figures (e.g. Figure 1B, and Figure 2). Among the different stains, VGlut2 revealed the most distinct cross layer cytoarchitectonic features [54; 97; 98]. In animals whose tissue sections were not available, we used the schematic map as described in [8; 50] for the identification of cortical areas.

Image alignment

The alignment of MRI and histology images was performed by identification of corresponding anatomical landmarks in each structural image such as the visible sulci, ventricles, and overall shape of deep brain structures such as the thalamus. These coordinates were then put into a point-based registration algorithm (implemented in MATLAB, details in ref. [17]) to align the two sets of images.

Results

Nociceptive heat data from eleven animals (twelve scans, one animal scanned twice) and tactile data from nine animals (nine scans) were analyzed and included in the generation of probability maps. BOLD signal changes to heat stimuli obtained from all animals (n = 11) were included in time course quantifications. Representative fMRI activation maps from three (out of eleven) animals are shown in Figures 2 and 4. Sample histological brain sections from two (out of seven total) animals are shown in Figures 1 and 2. To distinguish from the common usage of SII in both human and monkey literature, we labeled the classical SII region (part of parietal operculum) as S2 (secondary somatosensory area), PV (parietal ventral area), and VS (ventral somatosensory area) [51; 52] in our illustrations. Areas posterior to S2/PV and posterior insular (pIns) were classified as area 7b and retroinsular (Ri) area, respectively. In general, activations in regions of the lateral sulcus are labeled as S2, PV, VS, pIns, Ri and area 7b.

NIH-PA Author Manuscript

NIH-PA Author Manuscript

NIH-PA Author Manuscript

Distributed activation to nociceptive heat and tactile stimulation in regions around the lateral sulcus

Robust and statistically significant stimulus-related BOLD signal changes in response to unilateral noxious heat stimulation of the digits were found in cortical regions distributed along the lateral sulci in both hemispheres (Figure 2). Similar bilateral activation patterns were observed across animals as illustrated in the series of coronal slices from two animals (posterior to anterior slices, M1: A–J; M2: K–Y). Heat activation maps of M1 (Figure 2 A–J) were acquired at a higher in-plane resolution 0.35×0.35 mm^2. According to published cortical maps, as shown in Figure 3, we localized nociceptive heat stimulus evoked activations to bilateral S2/PV (green arrows) and contralateral VS (green arrows), pIns (indigo arrows), and Ri (light blue arrow). Differential histological staining of coronal brain sections in a subset (n = 7) of animals was used to account for inter-subject variability in brain anatomy and to identify activated cortical areas with better accuracy. VGluT2 (layer 4 afferent terminals) was found to be the best transcortical marker in revealing distinct cytoarchitectonic features of different cortical areas. As shown in subject M2 (Figure 2 P–T), the dense middle layer staining in S2/PV – VS – pIns and the light staining in neighboring area 1–2, area 7b and Ri further confirm the identification of nociceptive heat activation in bilateral S2/PV, VS, pIns, area 7b (red arrows), and contralateral Ri. While small anatomical differences were observed to exist across animals, cortical areas identified with individual histology were in general agreement with the published map for this region (Left column in Figure 5; for details see [8; 50]).

Within an individual cortical region (e.g. bilateral S2/PV on the upper bank of the lateral sulcus), there were multiple activation peaks (bright color patches in Figure 2B and 2L), concurring with a previous report on contralateral SI activation with identical stimulation [13]. Compared to nociceptive heat stimulation (Figure 2A – E and K – O), innocuous tactile stimulation evoked responses in fewer cortical areas and to a significantly less extent spatially in general (Figure 2F – J and U – Y). For example, activation in response to tactile stimulation was absent in area 7b in M1 and M2. The spatial relationship between activation in response to nociceptive heat and tactile stimulation varied across areas. Activation to both stimuli was similar across animals on the upper bank of the lateral sulcus (S2/PV in Figure 2 B, G, L, V). At more anterior locations (Figure 2 C, H, M, W), responses appeared at different sites. To summarize, while inter-subject variations were present, there was a high degree of consistency across subjects in both the nociceptive heat and tactile evoked activation.

Different activation frequencies in contralateral and ipsilateral hemispheres

The reliability of bilateral activation across animals, regardless of the specific physical location was evaluated by activation frequency at different cortical areas at the population level (n = 12) and animals (n = 11) as summarized in Table 1. With a criterion of 50% or greater activation frequency, 10 areas in both hemispheres were identified as responsive to nociceptive stimulation. In comparison, only four areas (bilateral S2/PV, ipsilateral VS and Ri) were classified as responsive to innocuous tactile stimulation.

Nociceptive heat stimulation activated contralateral areas at higher frequencies than ipsilateral areas. The most consistent activation was observed in contralateral S2/PV (83%) and VS (83%). Interestingly, activation frequencies of ipsilateral areas were in general higher than the corresponding contralateral areas under tactile stimulus conditions. The most commonly activated cortical areas to tactile stimulation included bilateral S2/PV (67% for contralateral and 78% for ipsilateral hemisphere). Bilateral S2/PV regions seemed to be the most consistently activated cortical area in response to both nociceptive heat and tactile stimuli. The largest activation frequency difference was observed in bilateral pIns, which

NIH-PA Author Manuscript

NIH-PA Author Manuscript

NIH-PA Author Manuscript

was activated in 58% of scans (7/12) during nociceptive heat stimulation, but in only 22% (contralateral, 2/9) to 33% (ipsilateral, 3/9) of scans during tactile stimulation.

Probability maps were generated to evaluate the reproducibility and variations of activation at each particular cortical location at the population level (Figure 3). The probability of activation in each cluster was color-coded. Due to the large difference between stimuli in activation frequency, we used different colorcoded scales for nociceptive heat (A–E) and tactile (F–J) conditions. In the nociceptive heat condition, dark red indicates the highest activation frequency (92%, 11 out of 12 scans) while yellow indicates a threshold activation frequency of 50% (6 out of 12 scans) (see scale bar next to Figure 3E). For display purposes, a 50% threshold was arbitrarily chosen. With this criterion, multiple activation clusters were found in the upper bank along the sylvian fissure of the two hemispheres, the fundus (the cortex strip along the inner side of lateral sulcus) and the tale region of the lateral sulcus (the posterior end of the lateral sulcus), and in insular cortex. Contralateral to the side of stimulation, activation in response to nociceptive heat stimulation was present in all five slices (Figure 3 A–E). On the most posterior slice (according to the cytoarchitectonically defined cortical areas [8; 50] and the topographic map [52] in squirrel monkeys) two clusters (red circles) were identified to be within area 7b (Figure 3A). On the following four slices (Figure 3 B–E), activation clusters were located in S2/PV (Figure 3 B & C), VS (Figure 3D), the medial activation cluster at the fundus of the lateral sulcus, pIns (indigo circles in Figure 3E) and Ri (light blue circle in Figure 3 B&C, located posterior to insula at the tail region of the lateral sulcus). Activation in contralateral Ri (67%), and ipsilateral pIns (58%) is not shown on the probability map because of significant variation in the location across animals.

In the tactile stimulation condition, activation frequency at each location was much lower than that observed during nociceptive heat stimulation. On the contralateral side, S2/PV activation to heat stimulation spanned across three consecutive image slices (Figure 3 B–D) while S2/PV activation in response to tactile stimulation (using a 44% activation criterion) was contained to one slice (Figure 3I). On the ipsilateral side, two separate activation clusters appeared in S2/PV, located in posterior (Figure 3 B & G) and anterior image slices (Figure 3E, I & J) in both heat and tactile stimulus conditions. In contrast to nociceptive heat stimulation, activation in response to the tactile stimulus in S2/PV region was located in more anterior locations (comparing activation clusters in I & J with activation clusters in B–E).

To summarize, multiple areas in the parasylvian region were responsive to nociceptive heat and tactile stimuli. In general, nociceptive responses in contralateral cortical areas were more robust than ipsilateral cortical areas as indicated by activation frequency and consistency of activation location across subjects. A nociceptive stimulus responsive network included bilateral areas in the S2/PV, VS, pIns and Ri regions. Activation response frequency to tactile stimulation was similar to the heat nociceptive condition in bilateral S2/PV area, but was significantly less in other areas (ipsilateral Vs and Ri). The greatest difference between heat and tactile activation frequency occurred in the posterior insular cortex and area 7b (Table 1), suggesting preferential roles in nociceptive processing in these areas.

Differential BOLD signal time courses in bilateral cortical areas

The magnitude and temporal differences of BOLD signal changes at different cortical regions were further evaluated to examine potential functional differences of each activated area during the processing of nociceptive input. Specifically, an ROI-based time course analysis was conducted in individual animals. The response profile at each cortical region was then quantified across animals (Figure 5). Figure 4 illustrates single-trial changes in BOLD signal (black curves) of single voxels at stimulus-responsive and control locations

NIH-PA Author Manuscript

NIH-PA Author Manuscript

NIH-PA Author Manuscript

(color boxes in Figure 4 A & F) during stimulus on (yellow shadow blocks in Fig 4 B–E and G–M) and off cycles (white intervals) in animal M3. The observed BOLD signal changes of 0.4% to 0.8% were comparable to previous 9.4T fMRI measures in anesthetized animals [17; 101]. At control locations in both hemispheres, BOLD signal fluctuated at low magnitude and in a non-stimulus related fashion (Figure 4 D, E, L and M). The correlation between BOLD signal time course and stimulus presentation (nine to eighteen repeats) is statistically significant at $p<10^{-4}$ without multiple comparison and at $p<0.05$ with multiple comparison. Additionally, the amplitude of BOLD signal change during the stimulation is significantly higher ($p<0.01$, t-test) than that during the rest (defined as the 3 frames prior to stimulus onset).

The coronal imaging plane used in the present study allowed us to quantify inter-hemispheric differences in magnitude and temporal profiles of responses to the nociceptive stimulus (Figures 4 and 5). Close examination of BOLD time courses (Figure 5) revealed several features. First, the duration of the BOLD response to the thermal nociceptive stimulus varied from one region to another. For instance, the contralateral S2/PV (Figure 5A) showed a sustained response, whereas the contralateral Ri (Figure 5E) showed a transient response. Second, BOLD signal magnitudes and magnitude differences of corresponding ipsilateral - contralateral brain clusters were specific for each cortical area examined. For instance, the peak magnitudes of BOLD signal changes in contralateral VS (Figure 5B) and pIns (Figure 5F) were significantly greater than the signal changes in the corresponding ipsilateral areas; whereas, ipsilateral Ri responded with greater peak amplitude than the corresponding contralateral area (Figure 5E). The sequence of areas, from strongest to weakest activation in response to heat nociceptive stimulation was contralateral VS (0.61%), contralateral pIns (0.53%), and contralateral Ri (0.37%). Responses in areas S2/PV and area 7b showed no significant ipsi-/contralateral differences (Figure 5A & C). The descriptive and inferential statistics of the BOLD signal changes are detailed in Table 2. Third, among the parasylvian areas, the fastest peaking region was the contralateral Ri (TTP = 14.4 sec), while the slowest peaking regions were contralateral S2 (18.9 sec) and VS (18.6 sec). Statistically, however, these differences between the fastest and the slowest peaking areas were not significant (Figure 5D). Finally, the peak magnitudes of BOLD signal undershoot (signal decrease below the pre-stimulus baseline) in ipsilateral areas S2/PV (−0.21%) and 7b (−0.23%) were significantly greater than corresponding contralateral areas. In sum, across areas and hemispheres, the strongest responses to nociceptive heat stimulation were located in contralateral VS and S2/PV; whereas, the weakest but fasted response was in the contralateral Ri. At control locations, BOLD signals either increased or decreased but in small magnitude and with large intertrial variations. These changes were not statistically significant; therefore, we interpret them as stimulusunrelated intrinsic BOLD signal fluctuations.

Schematic summary of the nociceptive and tactile processing networks

The present study found differences in fMRI activation responses to nociceptive heat stimulation and an innocuous tactile stimulation in cortical areas around the parasylvian region (52, 64) in squirrel monkeys. The findings of the study are summarized in two schematic illustrations[50; 52] based on available fMRI and histological information (Figure 6). Due to technique constraints, the present study did not examine the anterior insular cortex, and as such, the illustrations do not include the anterior insular region. The side-by-side arrangement of the two schematic drawings illustrates that the reliability of activation in different cortical regions varies. For example, the functional and structural organization and inter-areal borders of the operculo-insular (e.g. border between VS and posterior insula) and its posterior region at the tail of the lateral sulcus, where areas 5, 7b, and Ri reside, have not been fully established, particularly in New World monkeys. To simplify we refer to the

NIH-PA Author Manuscript

NIH-PA Author Manuscript

NIH-PA Author Manuscript

region posterior to S2/PV on the upper bank of the lateral sulcus as area 7b, and the region posterior to insular cortex on the lower bank of the lateral sulcus as Ri. Activation probability estimation along with histological evidence demonstrated that bilateral S2/PV and ipsilateral VS and Ri areas were responsive to unilateral noxious heat and innocuous tactile stimuli. Bilateral posterior insular (pIns) and area 7b, and contralateral VS and Ri responded preferentially to nociceptive heat stimulation.[3; 6; 34; 60; 86; 95] The present study revealed a more detailed and complex processing network for nociceptive heat and innocuous tactile inputs compared with the recently identified pain activation regions (subregions of SII, posterior and anterior insular cortices) in human fMRI literature [3; 6; 34; 60; 86; 95]. We cannot determine the functional specificity of these areas to nociceptive heat stimuli since we only tested cortical responses to a single noxious temperature. Future studies should test a range of stimulus conditions from innocuous to highly noxious stimuli (e.g. [16]). Nevertheless, our findings indicate a more bilateral cortical network for processing nociceptive heat input as compared to human studies.

Discussion

Involvements of bilateral SII region (S2/PV and VS) in nociceptive and tactile processing

The present study found activation of the S2/PV region (commonly classified as SII, located on the upper bank of the lateral sulcus) in response to both noxious heat and touch, consistent with the existing evidence in humans and animals [11; 26; 31–33; 43; 63; 84; 100] reviews see [1; 71]. This activation pattern is supported by neuronal electrical activity studies where a small proportion of thermal and/or mechanical nociceptive neurons have been isolated from low threshold mechanical neuron clusters in the posterior portion of SII and area 7b [18; 19; 27; 28; 78]. Our observation of a posteriorly shifted fMRI response to heat stimulus, is in agreement with electrophysiological evidence from monkeys and fMRI evidence from humans [34; 35; 86]. The property of bilateral receptive fields of both nociceptive and tactile neurons in this posterior region may mediate the observed bilateral fMRI activation in response to unilateral stimulation.

Although functional specificity of S2 and the parietal-ventral region (PV) in touch processing remains to be determined, existing anatomical evidence from cytoarchitectonic and tract - tracing studies as well as electrophysiological evidence of two distinct somatotopic maps strongly support that S2 and PV are two separate parasylvian structures in non-human primates. Compared to the well-documented functions of S2 and PV in touch processing, the existence and functional role of VS is still debatable [9, 10, 20, 23, 52, 53, 55]. In the present study, close examination of the activation pattern actually reveals two separate activation clusters for heat and tactile stimulation in anterior to posterior locations that is more apparent in the ipsilateral than contralateral hemisphere. Because finger representations in the S2 and PV are organized in a mirror finger-to-finger manner [20; 55; 56], the observed separation does not likely reflect separate activation foci in S2 and PV, but rather a modular organization within a single cortical area or activations in two separated areas; likely S2/PV and VS. The activation localization precision in anterior – posterior orientation is compromised in the present study due to the plane of sectioning, and therefore, further systematic somatotopic mapping is needed to confirm or disapprove the separation of nociceptive and tactile responses.

It is possible that difference in the extent of nociceptive and tactile activations could at least partially be due to a difference in stimulus size. However, the spatial separation of heat and tactile activation centers should not be a result of difference in stimulus sizes because the stimulating sites are overlapped. Furthermore, limited by its nature, BOLD signals are incapable of determining whether signals are generated from a cluster of functionally related neurons or scattered neurons within a region. FMRI signals to nociceptive stimulation could

NIH-PA Author Manuscript

NIH-PA Author Manuscript

NIH-PA Author Manuscript

originate from both nociceptive and non-nocieptive neurons [24]. Thus, further functional characterization of nociceptive neurons in these regions is essential for determining the specific functions of these regions. Nevertheless, our findings support the involvements of bilateral S2/PV region in processing noxious heat and innocuous tactile inputs.

Distinct activation in response to noxious heat and innocuous touch in posterior parasylvanian regions

Nociceptive heat stimulation activated more cortical areas than tactile stimulation in the posterior region around the lateral sulcus. Bilateral posterior insula (pIns) and area 7b responded preferentially to nociceptive stimulation. This finding supports recent human fMRI results, showing that pain-related activation and somatotopic organization are observed in the posterior insular region [3; 92]. In addition, direct stimulation to the posterior insular region has been shown to elicit pain sensation [69]. The functional role of the posterior insular region (possibly including SII and area 7b as well) in the generation of subjective pain sensation has been implicated by findings from recent lesion studies [48; 94]. Moreover, the observed response in area 7b to nociceptive stimulation is supported by electrophysiological evidence in monkeys [27; 28]. The low activation frequency of area 7b in response to tactile stimulation is a bit surprising due to the large number of low threshold mechanical neurons identified in this region in awake monkeys [27; 46]. This soamtosensory association region has been considered as a high order integrative area, and it is therefore possible that anesthesia produced strong suppressive effects on fMRI signals, particularly nociceptive signals. In sum, the present study bolsters evidence for a role of the pIns and area 7b in nociceptive heat processing by providing fMRI findings in monkeys for the first time. The current study found significantly stronger inter-hemisphere response differences in pain processing (greater BOLD magnitude) in both contralateral areas (VS and pins) and ipsilateral area (Ri) (Figure 5) compared to previous reports [1; 65; 80]. While some degree of hemisphere dominance for certain aspects of pain sensation has been reported in humans [80; 99], whether the same organization exists in monkeys and the functional significance of these inter-hemispheric differences need to be further explored.

The fastest peaking response to nociceptive stimulation was observed in the contralateral Ri. The inter-areal differences in time to peak, however, were not statistically significant. The average time to peak (17.35 sec) in the current study was quite slow and may be due to a variety of factors. One possible factor relates to the block design used in the present study. The peak BOLD was calculated as an accumulated response over a long period of stimulation (24 sec). Another factor may relate to the use of glabrous skin, a skin type containing a large number of slow peaking nociceptors [89]. A third factor may relate to the delivery of long-duration heat stimulation though a contact thermode. With this type of stimulus (temperature was ramped at 70° C/sec and plateaued 1 sec after stimulus onset), human subjects often report slow-onset pain sensation starting around 7–8 sec after stimulus onset (our own unpublished observations, [45; 87]. This slow increase in pain sensation may reflect a temporal summation of pain perception [87]. In sum, the findings from the present study not only confirmed the roles of bilateral S2/PV in processing both noxious heat and tactile stimulation, but also identified two nociceptive preferential regions: bilateral pIns and area 7b. The contralateral VS and Ri shared similar responses to nociceptive heat and touch stimuli.

Identification of the different parasylvian structures is important for understanding nociceptive processing pathways. Determination of different parasylvian structures is based on multiple criteria including cytoarchitectonic feature, anatomical connectivity circuitry and properties of neuronal responses in non-human primates [68]. Thus, localization of nociceptive responses to different parasylvian structures will further help us to identify brain circuitries that are responsible for pain perception [36; 57].

NIH-PA Author Manuscript

NIH-PA Author Manuscript

NIH-PA Author Manuscript

We recognize that anesthetics in general have suppressive effects on brain functional signals such as intrinsic optical and BOLD signals [14; 15; 103]. Compared to awake preparations, neuronal and functional responses in anesthetized conditions typically are smaller in amplitudes, but are not significantly different in temporal profiles. It is also possible that anesthetic may have differential effects on different parasylvain areas since it has long been recognized that higher order cortical areas are more sensitive to anesthesia.

Issues related to identification of cortical areas

Accurately identifying cortical areas and assigning fMRI activation to different cortical areas within the parasylvian region are critical components of the present study. We implemented two procedures to ensure accurate alignment between histological sections and MRI images. First, we placed coronal MRI structural images in a stereotactic framework. Second, upon the completion of the functional study, we cut brain tissue in the coronal plain and processed for histology. Despite these efforts, there was variability in the accuracy of identification across cortical areas. For example, the assignment of VS activation in response to nociceptive stimulation is open to argument. Based on available histological and structural MRI information, we classified areas near the fundus of the lateral sulcus as VS. Compared to macaque monkeys, the cytoarchitectonic features that can be used to determine inter-areal borders between parietal operculum and insula were not robust. Therefore, it is possible that activation localized to the VS in the current study may be equivalent to activation observed in the dorsal posterior part of granular insular region of macaques. Despite the uncertainty of precise identification of each area, the current fMRI results support the involvement of more than one area within the bilateral parietal operculum region and the posterior portion of the lateral sulcus in the processing of nociceptive stimulation while tactile inputs are processed within a subset of the regions activated by nociception.

In conclusion, the present study provides fMRI evidence supporting the involvement of bilateral S2/PV, VS, Ri, Ins and area 7b in the processing of nociceptive information in monkeys. Innocuous tactile input on the other hand, were processed only in a subset of nociceptive responsive regions including bilateral S2/PV and ipsilateral VS and Ri. This study establishes the foundation for future studies aimed at the identification of nociceptive-specific processing circuitry and for the examination of neuronal mechanisms underlying pain processing.

Acknowledgments

We thank Dr. Allen Newton for providing Matlab script for generating activation frequency maps. This work is supported by NIH grant R21 DA024831 to LMC. We declare that our research was conducted in accordance with the ‘statement of ethical standards’. Vanderbilt University IACUC approved all the procedures described in this manuscript.

Reference

1. Apkarian AV, Bushnell MC, Treede RD, Zubieta JK. Human brain mechanisms of pain perception and regulation in health and disease. Eur J Pain. 2005; 9(4):463–484. [PubMed: 15979027]
2. Asplund CL, Todd JJ, Snyder AP, Marois R. A central role for the lateral prefrontal cortex in goal-directed and stimulus-driven attention. Nat Neurosci. 2010; 13(4):507–512. [PubMed: 20208526]
3. Baumgartner U, Iannetti GD, Zambreanu L, Stoeter P, Treede RD, Tracey I. Multiple somatotopic representations of heat and mechanical pain in the operculo-insular cortex: a high-resolution fMRI study. J Neurophysiol. 2010; 104(5):2863–2872. [PubMed: 20739597]
4. Birklein F, Rolke R, Muller-Forell W. Isolated insular infarction eliminates contralateral cold, cold pain, and pinprick perception. Neurology. 2005; 65(9):1381. [PubMed: 16275823]

NIH-PA Author Manuscript

NIH-PA Author Manuscript

NIH-PA Author Manuscript

5. Bjornsdotter M, Loken L, Olausson H, Vallbo A, Wessberg J. Somatotopic organization of gentle touch processing in the posterior insular cortex. J Neurosci. 2009; 29(29):9314–9320. [PubMed: 19625521]
6. Bornhovd K, Quante M, Glauche V, Bromm B, Weiller C, Buchel C. Painful stimuli evoke different stimulus-response functions in the amygdala, prefrontal, insula and somatosensory cortex: a singletrial fMRI study. Brain. 2002; 125(Pt 6):1326–1336. [PubMed: 12023321]
7. Bowsher D, Brooks J, Enevoldson P. Central representation of somatic sensations in the parietal operculum (SII) and insula. Eur Neurol. 2004; 52(4):211–225. [PubMed: 15539775]
8. Burton H, Jones EG. The posterior thalamic region and its cortical projection in New World and Old World monkeys. J Comp Neurol. 1976; 168(2):249–301. [PubMed: 821975]
9. Burton H, Robinson CJ. Responses in the first or second somatosensory cortical area in cats during transient inactivation of the other ipsilateral area with lidocaine hydrochloride. Somatosens Res. 1987; 4(3):215–236. [PubMed: 3563198]
10. Burton H, Sinclair RJ, Hong SY, Pruett JR Jr, Whang KC. Tactile-spatial and cross-modal attention effects in the second somatosensory and 7b cortical areas of rhesus monkeys. Somatosens Mot Res. 1997; 14(4):237–267. [PubMed: 9443366]
11. Burton H, Sinclair RJ, Wingert JR, Dierker DL. Multiple parietal operculum subdivisions in humans: tactile activation maps. Somatosens Mot Res. 2008; 25(3):149–162. [PubMed: 18821280]
12. Burton H, Videen TO, Raichle ME. Tactile-vibration-activated foci in insular and parietal-opercular cortex studied with positron emission tomography: mapping the second somatosensory area in humans. Somatosens Mot Res. 1993; 10(3):297–308. [PubMed: 8237217]
13. Chen LM, Dillenburger BC, Wang F, Friedman RM, Avison MJ. High-resolution functional magnetic resonance imaging mapping of noxious heat and tactile activations along the central sulcus in New World monkeys. Pain. 2011; 152(3):522–532. [PubMed: 21177033]
14. Chen LM, Friedman RM, Ramsden BM, LaMotte RH, Roe AW. Fine-scale organization of SI (area 3b) in the squirrel monkey revealed with intrinsic optical imaging. J Neurophysiol. 2001; 86(6):3011–3029. [PubMed: 11731557]
15. Chen LM, Friedman RM, Roe AW. Optical imaging of SI topography in anesthetized and awake squirrel monkeys. J Neurosci. 2005; 25(33):7648–7659. [PubMed: 16107651]
16. Chen LM, Friedman RM, Roe AW. Area-specific representation of mechanical nociceptive stimuli within SI cortex of squirrel monkeys. Pain. 2009; 141(3):258–268. [PubMed: 19136211]
17. Chen LM, Turner GH, Friedman RM, Zhang N, Gore JC, Roe AW, Avison MJ. High-resolution maps of real and illusory tactile activation in primary somatosensory cortex in individual monkeys with functional magnetic resonance imaging and optical imaging. J Neurosci. 2007; 27(34):9181–9191. [PubMed: 17715354]
18. Chudler EH, Dong WK, Kawakami Y. Tooth pulp-evoked potentials in the monkey: cortical surface and intracortical distribution. Pain. 1985; 22(3):221–233. [PubMed: 4034222]
19. Chudler EH, Dong WK, Kawakami Y. Cortical nociceptive responses and behavioral correlates in the monkey. Brain Res. 1986; 397(1):47–60. [PubMed: 3801865]
20. Coq JO, Qi H, Collins CE, Kaas JH. Anatomical and functional organization of somatosensory areas of the lateral fissure of the New World titi monkey (Callicebus moloch). J Comp Neurol. 2004; 476(4):363–387. [PubMed: 15282711]
21. Craig AD. A new view of pain as a homeostatic emotion. Trends Neurosci. 2003; 26(6):303–307. [PubMed: 12798599]
22. Craig AD, Chen K, Bandy D, Reiman EM. Thermosensory activation of insular cortex. Nat Neurosci. 2000; 3(2):184–190. [PubMed: 10649575]
23. Cusick CG, Wall JT, Felleman DJ, Kaas JH. Somatotopic organization of the lateral sulcus of owl monkeys: area 3b, S-II, and a ventral somatosensory area. J Comp Neurol. 1989; 282(2):169–190. [PubMed: 2496153]
24. Davis KD. Neurophysiological and anatomical considerations in functional imaging of pain. Pain. 2003; 105(1–2):1–3. [PubMed: 14499413]
25. Davison, AC.; Hinkley, DV. Bootstrap methods and their application. Cambridge University Press; 1998.

NIH-PA Author Manuscript

NIH-PA Author Manuscript

NIH-PA Author Manuscript

26. Disbrow E, Roberts T, Krubitzer L. Somatotopic organization of cortical fields in the lateral sulcus of Homo sapiens: evidence for SII and PV. J Comp Neurol. 2000; 418(1):1–21. [PubMed: 10701752]
27. Dong WK, Chudler EH, Sugiyama K, Roberts VJ, Hayashi T. Somatosensory, multisensory, and task-related neurons in cortical area 7b (PF) of unanesthetized monkeys. J Neurophysiol. 1994; 72(2):542–564. [PubMed: 7983518]
28. Dong WK, Salonen LD, Kawakami Y, Shiwaku T, Kaukoranta EM, Martin RF. Nociceptive responses of trigeminal neurons in SII-7b cortex of awake monkeys. Brain Res. 1989; 484(1–2): 314–324. [PubMed: 2713690]
29. Duong TQ, Kim DS, Ugurbil K, Kim SG. Spatiotemporal dynamics of the BOLD fMRI signals: toward mapping submillimeter cortical columns using the early negative response. Magn Reson Med. 2000; 44(2):231–242. [PubMed: 10918322]
30. Duong TQ, Kim DS, Ugurbil K, Kim SG. Localized cerebral blood flow response at submillimeter columnar resolution. Proc Natl Acad Sci U S A. 2001; 98(19):10904–10909. [PubMed: 11526212]
31. Eickhoff SB, Amunts K, Mohlberg H, Zilles K. The human parietal operculum. II. Stereotaxic maps and correlation with functional imaging results. Cereb Cortex. 2006; 16(2):268–279. [PubMed: 15888606]
32. Eickhoff SB, Grefkes C, Zilles K, Fink GR. The somatotopic organization of cytoarchitectonic areas on the human parietal operculum. Cereb Cortex. 2007; 17(8):1800–1811. [PubMed: 17032710]
33. Eickhoff SB, Schleicher A, Zilles K, Amunts K. The human parietal operculum. I. Cytoarchitectonic mapping of subdivisions. Cereb Cortex. 2006; 16(2):254–267. [PubMed: 15888607]
34. Ferretti A, Babiloni C, Gratta CD, Caulo M, Tartaro A, Bonomo L, Rossini PM, Romani GL. Functional topography of the secondary somatosensory cortex for nonpainful and painful stimuli: an fMRI study. Neuroimage. 2003; 20(3):1625–1638. [PubMed: 14642473]
35. Ferretti A, Del Gratta C, Babiloni C, Caulo M, Arienzo D, Tartaro A, Rossini PM, Romani GL. Functional topography of the secondary somatosensory cortex for nonpainful and painful stimulation of median and tibial nerve: an fMRI study. Neuroimage. 2004; 23(3):1217–1225. [PubMed: 15528121]
36. Friedman DP, Murray EA, O'Neill JB, Mishkin M. Cortical connections of the somatosensory fields of the lateral sulcus of macaques: evidence for a corticolimbic pathway for touch. J Comp Neurol. 1986; 252(3):323–347. [PubMed: 3793980]
37. Frot M, Garcia-Larrea L, Guenot M, Mauguiere F. Responses of the supra-sylvian (SII) cortex in humans to painful and innocuous stimuli. A study using intra-cerebral recordings. Pain. 2001; 94(1):65–73. [PubMed: 11576746]
38. Frot M, Magnin M, Mauguiere F, Garcia-Larrea L. Human SII and posterior insula differently encode thermal laser stimuli. Cereb Cortex. 2007; 17(3):610–620. [PubMed: 16614165]
39. Frot M, Mauguiere F. Dual representation of pain in the operculo-insular cortex in humans. Brain. 2003; 126(Pt 2):438–450. [PubMed: 12538410]
40. Fukuda M, Moon CH, Wang P, Kim SG. Mapping iso-orientation columns by contrast agent-enhanced functional magnetic resonance imaging: reproducibility, specificity, and evaluation by optical imaging of intrinsic signal. J Neurosci. 2006; 26(46):11821–11832. [PubMed: 17108155]
41. Fukuda M, Wang P, Moon CH, Tanifuji M, Kim SG. Spatial specificity of the enhanced dip inherently induced by prolonged oxygen consumption in cat visual cortex: implication for columnar resolution functional MRI. Neuroimage. 2006; 30(1):70–87. [PubMed: 16257237]
42. Garcia-Larrea L, Perchet C, Creac'h C, Convers P, Peyron R, Laurent B, Mauguiere F, Magnin M. Operculo-insular pain (parasylvian pain): a distinct central pain syndrome. Brain. 2010; 133(9): 2528–2539. [PubMed: 20724291]
43. Gelnar PA, Krauss BR, Sheehe PR, Szeverenyi NM, Apkarian AV. A comparative fMRI study of cortical representations for thermal painful, vibrotactile, and motor performance tasks. Neuroimage. 1999; 10(4):460–482. [PubMed: 10493903]
44. Greenspan JD, Lee RR, Lenz FA. Pain sensitivity alterations as a function of lesion location in the parasylvian cortex. Pain. 1999; 81(3):273–282. [PubMed: 10431714]

NIH-PA Author Manuscript

NIH-PA Author Manuscript

NIH-PA Author Manuscript

45. Hashmi JA, Davis KD. Effect of static and dynamic heat pain stimulus profiles on the temporal dynamics and interdependence of pain qualities, intensity, and affect. J Neurophysiol. 2008; 100(4):1706–1715. [PubMed: 18701756]
46. Hyvarinen J. Regional distribution of functions in parietal association area 7 of the monkey. Brain Res. 1981; 206(2):287–303. [PubMed: 7214136]
47. Iannetti GD, Zambreanu L, Cruccu G, Tracey I. Operculoinsular cortex encodes pain intensity at the earliest stages of cortical processing as indicated by amplitude of laser-evoked potentials in humans. Neuroscience. 2005; 131(1):199–208. [PubMed: 15680703]
48. Isnard J, Magnin M, Jung J, Mauguiere F, Garcia-Larrea L. Does the insula tell our brain that we are in pain? Pain. 2011; 152(4):946–951. [PubMed: 21277680]
49. Jain N, Florence SL, Kaas JH. Reorganization of Somatosensory Cortex After Nerve and Spinal Cord Injury. News Physiol Sci. 1998; 13:143–149. [PubMed: 11390778]
50. Jones EG, Burton H. Areal differences in the laminar distribution of thalamic afferents in cortical fields of the insular, parietal and temporal regions of primates. J Comp Neurol. 1976; 168(2):197–247. [PubMed: 821974]
51. Kaas JH. Evolution of somatosensory and motor cortex in primates. Anat Rec A Discov Mol Cell Evol Biol. 2004; 281(1):1148–1156. [PubMed: 15470673]
52. Kaas JH. The evolution of the complex sensory and motor systems of the human brain. Brain Res Bull. 2008; 75(2–4):384–390. [PubMed: 18331903]
53. Kaas JH, Collins CE. The organization of somatosensory cortex in anthropoid primates. Adv Neurol. 2003; 93:57–67. [PubMed: 12894401]
54. King CD, Wong F, Currie T, Mauderli AP, Fillingim RB, Riley JL 3rd. Deficiency in endogenous modulation of prolonged heat pain in patients with Irritable Bowel Syndrome and Temporomandibular Disorder. Pain. 2009; 143(3):172–178. [PubMed: 19278784]
55. Krubitzer L, Clarey J, Tweedale R, Elston G, Calford M. A redefinition of somatosensory areas in the lateral sulcus of macaque monkeys. J Neurosci. 1995; 15(5 Pt 2):3821–3839. [PubMed: 7751949]
56. Krubitzer LA, Kaas JH. The organization and connections of somatosensory cortex in marmosets. J Neurosci. 1990; 10(3):952–974. [PubMed: 2108231]
57. Kurth F, Eickhoff SB, Schleicher A, Hoemke L, Zilles K, Amunts K. Cytoarchitecture and Probabilistic Maps of the Human Posterior Insular Cortex. Cereb Cortex. 2009
58. Lenz FA, Rios M, Chau D, Krauss GL, Zirh TA, Lesser RP. Painful stimuli evoke potentials recorded from the parasylvian cortex in humans. J Neurophysiol. 1998; 80(4):2077–2088. [PubMed: 9772262]
59. Lui F, Duzzi D, Corradini M, Serafini M, Baraldi P, Porro CA. Touch or pain? Spatio-temporal patterns of cortical fMRI activity following brief mechanical stimuli. Pain. 2008
60. Maihofner C, Herzner B, Otto Handwerker H. Secondary somatosensory cortex is important for the sensory-discriminative dimension of pain: a functional MRI study. Eur J Neurosci. 2006; 23(5): 1377–1383. [PubMed: 16553798]
61. Maihofner C, Kaltenhauser M, Neundorfer B, Lang E. Temporo-spatial analysis of cortical activation by phasic innocuous and noxious cold stimuli--a magnetoencephalographic study. Pain. 2002; 100(3):281–290. [PubMed: 12467999]
62. Maldjian JA, Gottschalk A, Patel RS, Detre JA, Alsop DC. The sensory somatotopic map of the human hand demonstrated at 4 Tesla. Neuroimage. 1999; 10(1):55–62. [PubMed: 10385581]
63. Maldjian JA, Gottschalk A, Patel RS, Pincus D, Detre JA, Alsop DC. Mapping of secondary somatosensory cortex activation induced by vibrational stimulation: an fMRI study. Brain Res. 1999; 824(2):291–295. [PubMed: 10196461]
64. Mazzola L, Isnard J, Peyron R, Guenot M, Mauguiere F. Somatotopic organization of pain responses to direct electrical stimulation of the human insular cortex. Pain. 2009; 146(1–2):99–104. [PubMed: 19665303]
65. Naito E, Roland PE, Grefkes C, Choi HJ, Eickhoff S, Geyer S, Zilles K, Ehrsson HH. Dominance of the right hemisphere and role of area 2 in human kinesthesia. J Neurophysiol. 2005; 93(2): 1020–1034. [PubMed: 15385595]

NIH-PA Author Manuscript

NIH-PA Author Manuscript

NIH-PA Author Manuscript

66. Ohara S, Crone NE, Weiss N, Treede RD, Lenz FA. Amplitudes of laser evoked potential recorded from primary somatosensory, parasylvian and medial frontal cortex are graded with stimulus intensity. Pain. 2004; 110(1–2):318–328. [PubMed: 15275782]

67. Olausson H, Lamarre Y, Backlund H, Morin C, Wallin BG, Starck G, Ekholm S, Strigo I, Worsley K, Vallbo AB, Bushnell MC. Unmyelinated tactile afferents signal touch and project to insular cortex. Nat Neurosci. 2002; 5(9):900–904. [PubMed: 12145636]

68. Orban GA, Van Essen D, Vanduffel W. Comparative mapping of higher visual areas in monkeys and humans. Trends Cogn Sci. 2004; 8(7):315–324. [PubMed: 15242691]

69. Ostrowsky K, Magnin M, Ryvlin P, Isnard J, Guenot M, Mauguiere F. Representation of pain and somatic sensation in the human insula: a study of responses to direct electrical cortical stimulation. Cereb Cortex. 2002; 12(4):376–385. [PubMed: 11884353]

70. Petrovic P, Petersson KM, Ghatan PH, Stone-Elander S, Ingvar M. Pain-related cerebral activation is altered by a distracting cognitive task. Pain. 2000; 85(1–2):19–30. [PubMed: 10692599]

71. Peyron R, Frot M, Schneider F, Garcia-Larrea L, Mertens P, Barral FG, Sindou M, Laurent B, Mauguiere F. Role of operculoinsular cortices in human pain processing: converging evidence from PET, fMRI, dipole modeling, and intracerebral recordings of evoked potentials. Neuroimage. 2002; 17(3):1336–1346. [PubMed: 12414273]

72. Peyron R, Garcia-Larrea L, Gregoire MC, Convers P, Richard A, Lavenne F, Barral FG, Mauguiere F, Michel D, Laurent B. Parietal and cingulate processes in central pain. A combined positron emission tomography (PET) and functional magnetic resonance imaging (fMRI) study of an unusual case. Pain. 2000; 84(1):77–87. [PubMed: 10601675]

73. Ploner M, Gross J, Timmermann L, Schnitzler A. Pain processing is faster than tactile processing in the human brain. J Neurosci. 2006; 26(42):10879–10882. [PubMed: 17050725]

74. Ploner M, Schmitz F, Freund HJ, Schnitzler A. Parallel activation of primary and secondary somatosensory cortices in human pain processing. J Neurophysiol. 1999; 81(6):3100–3104. [PubMed: 10368426]

75. Qi HX, Kaas JH. Myelin stains reveal an anatomical framework for the representation of the digits in somatosensory area 3b of macaque monkeys. J Comp Neurol. 2004; 477(2):172–187. [PubMed: 15300788]

76. Rios M, Treede R, Lee J, Lenz FA. Direct Evidence of Nociceptive Input to Human Anterior Cingulate Gyrus and Parasylvian Cortex. Curr Rev Pain. 1999; 3(4):256–264. [PubMed: 10998681]

77. Robinson CJ, Burton H. Organization of somatosensory receptive fields in cortical areas 7b, retroinsula, postauditory and granular insula of M. fascicularis. J Comp Neurol. 1980; 192(1):69–92. [PubMed: 7410614]

78. Robinson CJ, Burton H. Somatic submodality distribution within the second somatosensory (SII), 7b, retroinsular, postauditory, and granular insular cortical areas of M. fascicularis. J Comp Neurol. 1980; 192(1):93–108. [PubMed: 7410615]

79. Robinson CJ, Burton H. Somatotopographic organization in the second somatosensory area of M. fascicularis. J Comp Neurol. 1980; 192(1):43–67. [PubMed: 7410613]

80. Schlereth T, Baumgartner U, Magerl W, Stoeter P, Treede RD. Left-hemisphere dominance in early nociceptive processing in the human parasylvian cortex. Neuroimage. 2003; 20(1):441–454. [PubMed: 14527605]

81. Seifert F, Maihofner C. Central mechanisms of experimental and chronic neuropathic pain: findings from functional imaging studies. Cell Mol Life Sci. 2009; 66(3):375–390. [PubMed: 18791842]

82. Strigo IA, Albanese MC, Bushnell MC, Duncan GH. Visceral and cutaneous pain representation in parasylvian cortex. Neurosci Lett. 2005; 384(1–2):54–59. [PubMed: 15905031]

83. Stringer EA, Chen LM, Friedman RM, Gatenby C, Gore JC. Differentiation of somatosensory cortices by high-resolution fMRI at 7 T. Neuroimage. 2011; 54(2):1012–1020. [PubMed: 20887793]

84. Taylor KS, Davis KD. Stability of tactile- and pain-related fMRI brain activations: An examination of threshold-dependent and threshold-independent methods. Hum Brain Mapp. 2008

NIH-PA Author Manuscript

NIH-PA Author Manuscript

NIH-PA Author Manuscript

85. Timmermann L, Ploner M, Haucke K, Schmitz F, Baltissen R, Schnitzler A. Differential coding of pain intensity in the human primary and secondary somatosensory cortex. J Neurophysiol. 2001; 86(3):1499–1503. [PubMed: 11535693]
86. Torquati K, Pizzella V, Babiloni C, Del Gratta C, Della Penna S, Ferretti A, Franciotti R, Rossini PM, Romani GL. Nociceptive and non-nociceptive sub-regions in the human secondary somatosensory cortex: an MEG study using fMRI constraints. Neuroimage. 2005; 26(1):48–56. [PubMed: 15862204]
87. Tran TD, Wang H, Tandon A, Hernandez-Garcia L, Casey KL. Temporal summation of heat pain in humans: Evidence supporting thalamocortical modulation. Pain. 2010; 150(1):93–102. [PubMed: 20494516]
88. Treede RD, Apkarian AV, Bromm B, Greenspan JD, Lenz FA. Cortical representation of pain: functional characterization of nociceptive areas near the lateral sulcus. Pain. 2000; 87(2):113–119. [PubMed: 10924804]
89. Treede RD, Meyer RA, Raja SN, Campbell JN. Evidence for two different heat transduction mechanisms in nociceptive primary afferents innervating monkey skin. J Physiol. 1995; 483(Pt 3): 747–758. [PubMed: 7776255]
90. Treede RD, Vogel H, Rios M, Krauss G, Lesser RP, Lenz FA. Pain-related evoked potentials from parasylvian cortex in humans. Electroencephalogr Clin Neurophysiol Suppl. 1999; 49:250–254. [PubMed: 10533119]
91. Trulsson M, Francis ST, Bowtell R, McGlone F. Brain activations in response to vibrotactile tooth stimulation: a psychophysical and FMRI study. J Neurophysiol. 2010; 104(4):2257–2265. [PubMed: 20668275]
92. Tseng MT, Tseng WY, Chao CC, Lin HE, Hsieh ST. Distinct and shared cerebral activations in processing innocuous versus noxious contact heat revealed by functional magnetic resonance imaging. Hum Brain Mapp. 2010; 31(5):743–757. [PubMed: 19823988]
93. Varian H. Bootstrap Tutorial. The Mathematica Journal. 2005; 9(4):768–775.
94. Veldhuijzen DS, Greenspan JD, Kim JH, Lenz FA. Altered pain and thermal sensation in subjects with isolated parietal and insular cortical lesions. Eur J Pain. 2010; 14(5):535. e531-511. [PubMed: 19939715]
95. Vogel H, Port JD, Lenz FA, Solaiyappan M, Krauss G, Treede RD. Dipole source analysis of laser-evoked subdural potentials recorded from parasylvian cortex in humans. J Neurophysiol. 2003; 89(6):3051–3060. [PubMed: 12783950]
96. Wong P, Kaas JH. Architectonic subdivisions of neocortex in the gray squirrel (Sciurus carolinensis). Anat Rec (Hoboken). 2008; 291(10):1301–1333. [PubMed: 18780299]
97. Wong P, Kaas JH. An architectonic study of the neocortex of the short-tailed opossum (Monodelphis domestica). Brain Behav Evol. 2009; 73(3):206–228. [PubMed: 19546531]
98. Wong P, Kaas JH. Architectonic subdivisions of neocortex in the Galago (Otolemur garnetti). Anat Rec (Hoboken). 2010; 293(6):1033–1069. [PubMed: 20201060]
99. Youell PD, Wise RG, Bentley DE, Dickinson MR, King TA, Tracey I, Jones AK. Lateralisation of nociceptive processing in the human brain: a functional magnetic resonance imaging study. Neuroimage. 2004; 23(3):1068–1077. [PubMed: 15528107]
100. Young JP, Herath P, Eickhoff S, Choi J, Grefkes C, Zilles K, Roland PE. Somatotopy and attentional modulation of the human parietal and opercular regions. J Neurosci. 2004; 24(23): 5391–5399. [PubMed: 15190112]
101. Zhang N, Gore JC, Chen LM, Avison MJ. Dependence of BOLD signal change on tactile stimulus intensity in SI of primates. Magn Reson Imaging. 2007; 25(6):784–794. [PubMed: 17614230]
102. Zhang N, Wang F, Turner GH, Gore JC, Avison MJ, Chen LM. Intra- and inter-subject variability of high field fMRI digit maps in somatosensory area 3b of new world monkeys. Neuroscience. 2010; 165(1):252–264. [PubMed: 19799969]
103. Zhao F, Jin T, Wang P, Kim SG. Isoflurane anesthesia effect in functional imaging studies. Neuroimage. 2007; 38(1):3–4. [PubMed: 17765574]

NIH-PA Author Manuscript

NIH-PA Author Manuscript

NIH-PA Author Manuscript

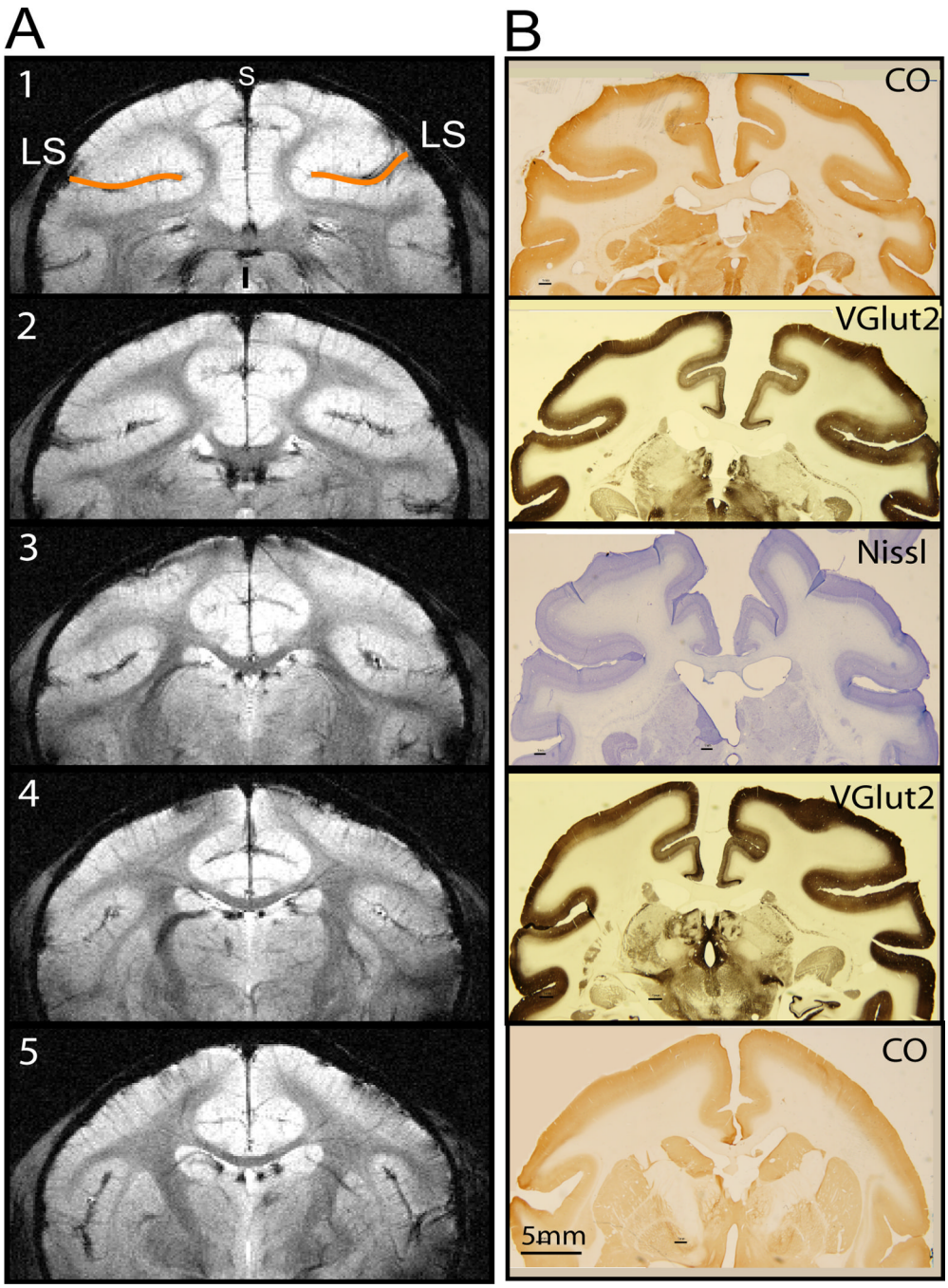

Figure 1.

High-resolution structural MRI images and corresponding histology of brain sections. A. Five T2* weighted structural MRI images. LS: lateral sulcus. Slice 1–5: posterior to anterior. s: superior. i: inferior. B. Corresponding tissue sections with various stains (VGlut2, CO and Nissl).

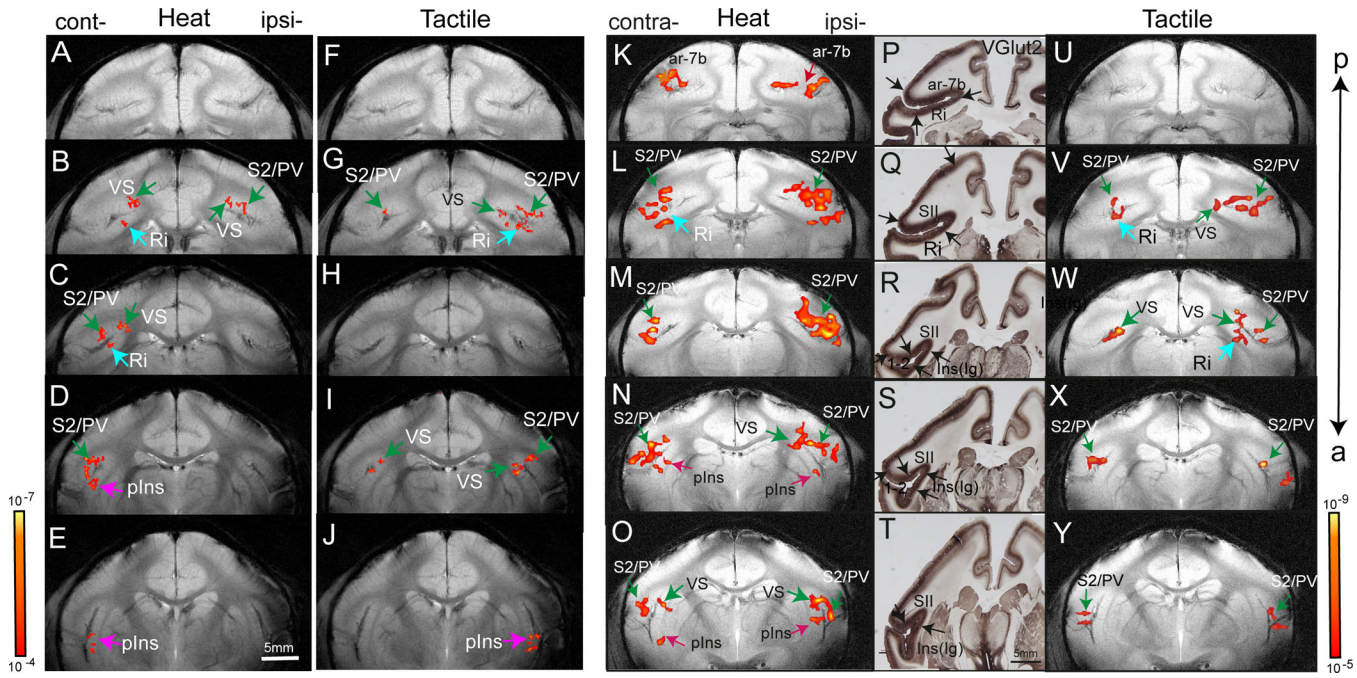

Figure 2.

Comparison of fMRI activation maps in response to nociceptive heat and tactile stimulation in two representative monkeys (M1 and M2). Nociceptive heat (47.5° C) (A–E, K–O) and 8 Hz tactile stimulation (FJ, U–Y) activation maps were overlaid on T2* weighted MRI structural images for display. FMRI activation maps were obtained in M1 at 0.35 × 0.35 mm^2 in plane resolution (threshold at $p \leq 10-4$ and a minimum voxel size of four) and in M2 at 0.7 × 0.7 mm^2 in plane resolution (threshold at $p \leq 10-5$ and a minimum voxel size of two). The p value ranges are indicated in two scale bars next to E and Y. P–T: Immunohistology for VGlut2 in corresponding brain sections. Black arrows indicate the transition area of the stain density of middle layers. Cont-: contralateral hemisphere. Ipsi-: ipsilateral hemisphere. ar-7b: area 7b. Ri: retroinsula. S2: second somatosensory area. PV: parietal ventral area. VS: ventral somatosensory area. pIns: posterior insular region. a: anterior. p: posterior.

NIH-PA Author Manuscript
NIH-PA Author Manuscript
NIH-PA Author Manuscript

NIH-PA Author Manuscript

NIH-PA Author Manuscript

NIH-PA Author Manuscript

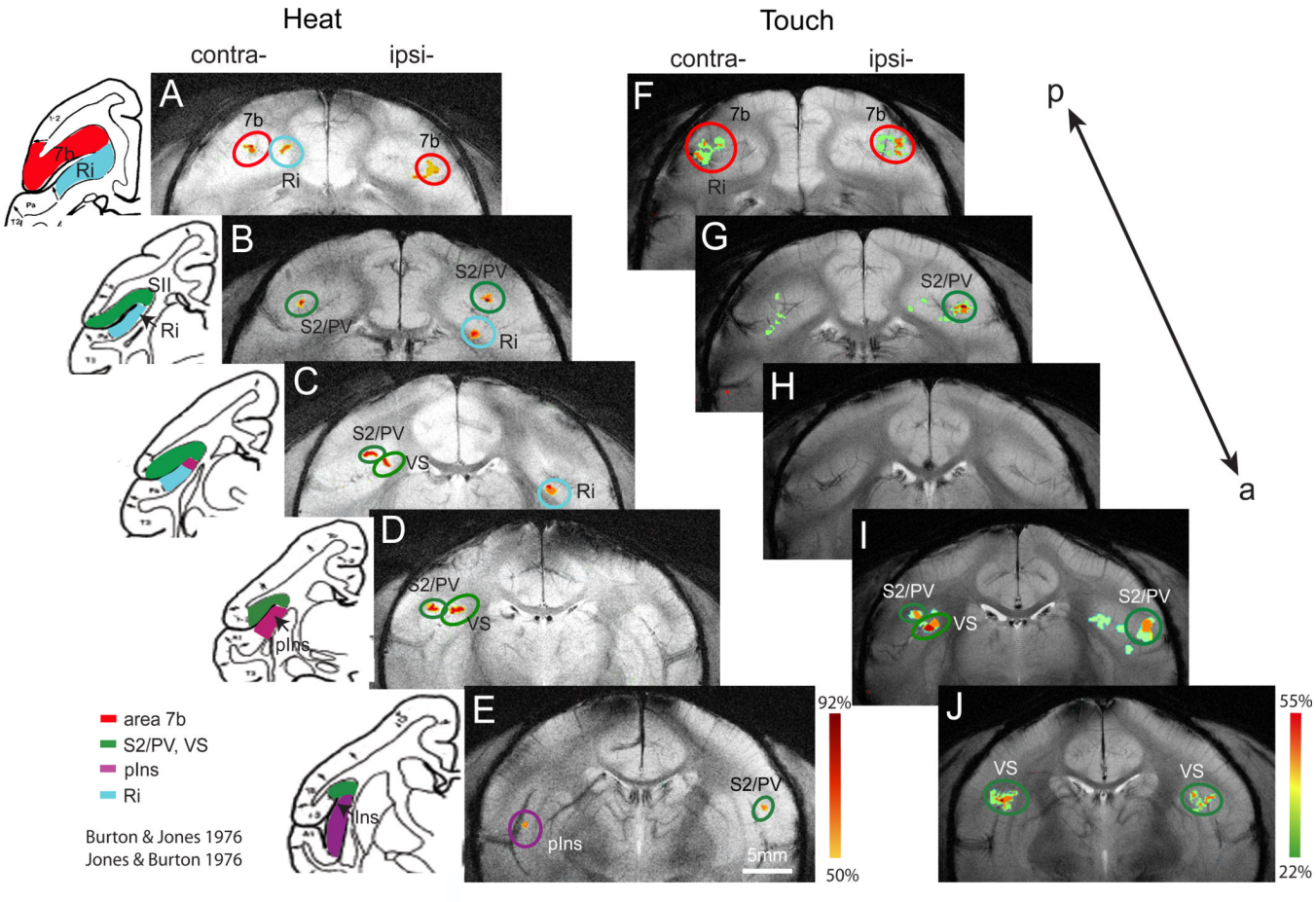

Figure 3.

Probability maps of activation in response to nociceptive heat and innocuous tactile stimulation. A–E. Activation frequency maps for nociceptive heat stimulation of fingers on five consecutive coronal image slices in posterior to anterior order. Color scale next to E indicates the frequency range (50% to 92%) of activation at each location. F–J. Activation frequency maps for innocuous tactile stimulation of fingers on five consecutive coronal image slices. Activation frequency ranges from 22% to 55% across animals (color scale next to J). Left inserts are corresponding schematic illustrations of the cortical areas and inter-areal borders identified by cytoarchitectural features of the brain tissue in the squirrel monkey (adapted and modified from Burton & Jones, 1976 and Jones & Burton, 1976). S2: secondary somatosensory area. PV: ventral parietal somatosensory area. VS: ventral somatosensory area. pIns: posterior insular cortex. Ri: retroinsular. 7b: area 7b.

NIH-PA Author Manuscript
NIH-PA Author Manuscript
NIH-PA Author Manuscript

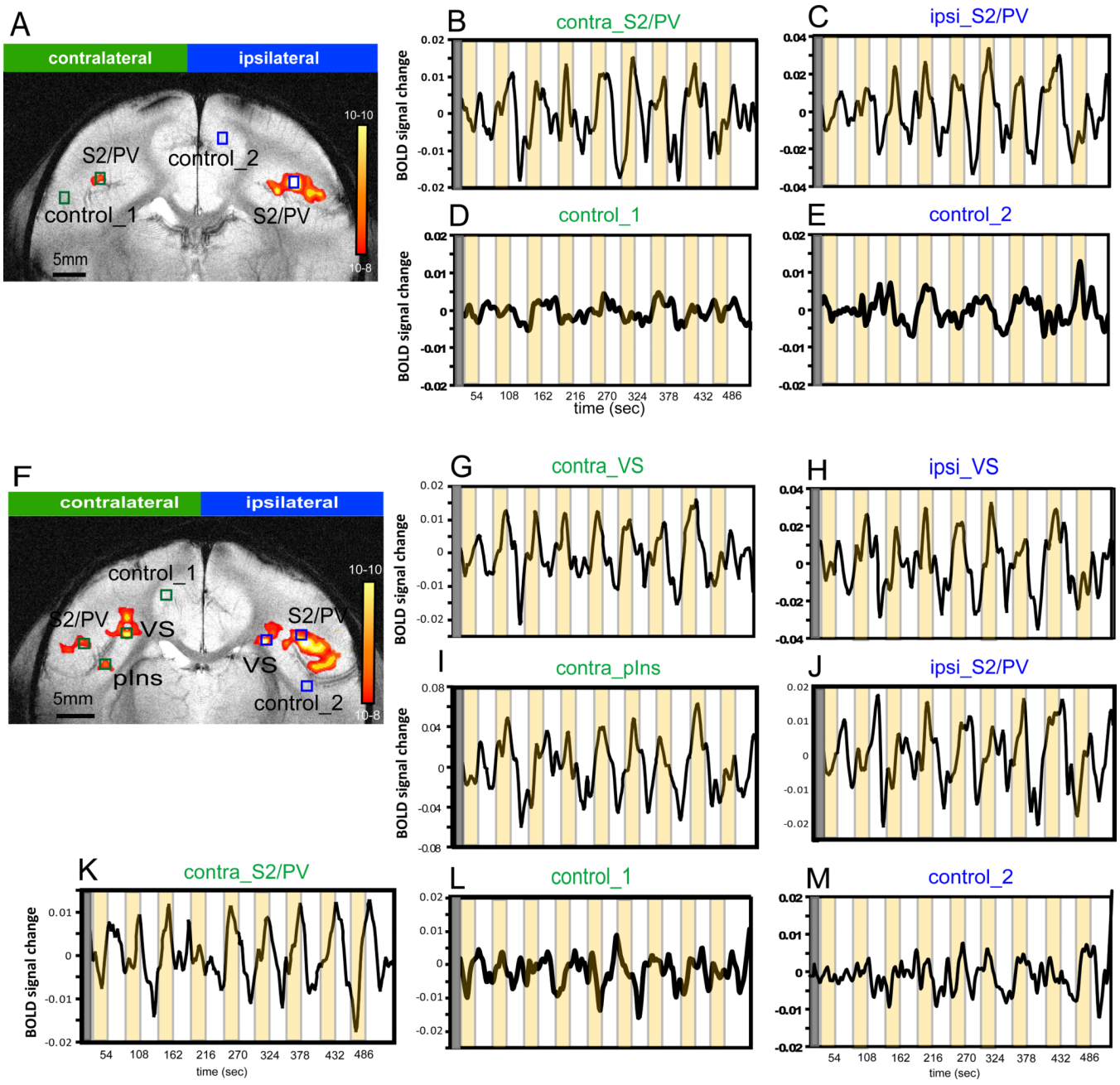

Figure 4.

Single trial BOLD signal plots of single voxels in different ROIs of slice 3 and slice 4 in a representative monkey (M3). A & B. Nociceptive heat stimulus evoked activation maps (threshold at a p-value of 1e-8 and a minimum voxel size of two). Peak response voxels are identified within each activation cluster for time course analysis. B, C, G–K. Single trial BOLD signal changes in contralateral and ipsilateral areas during heat stimulus on (24 sec, orange blocks) and off (30 sec, white intervals) cycles. D, E, L, M. BOLD signal changes in control locations during stimulus presentation. Y axis: arbitrary unit for BOLD signal changes.

NIH-PA Author Manuscript
NIH-PA Author Manuscript
NIH-PA Author Manuscript

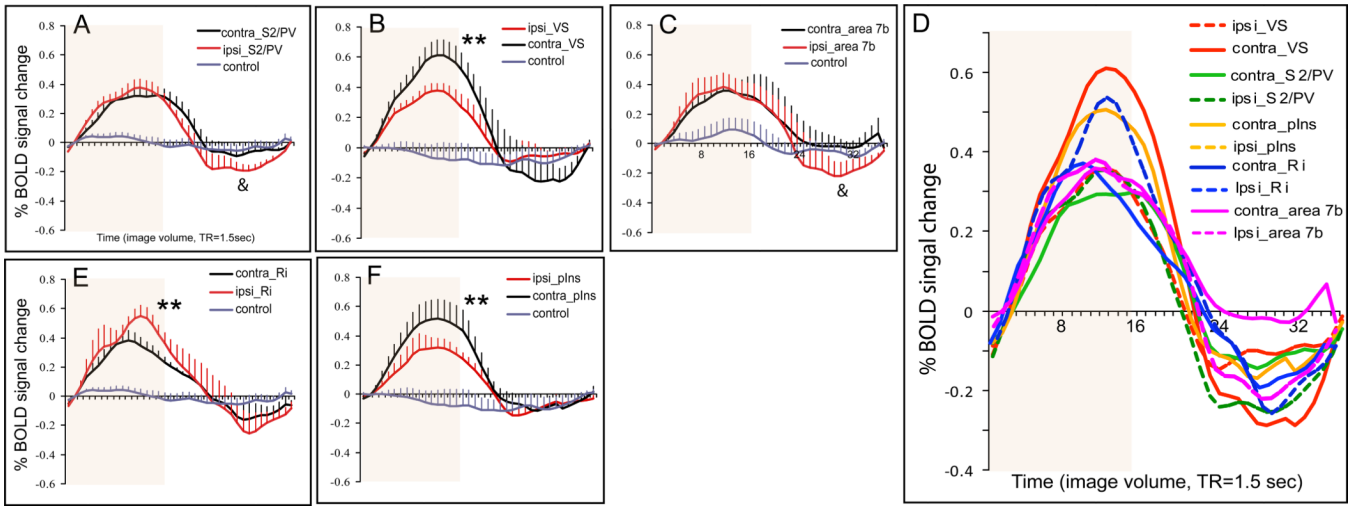

Figure 5.

Comparison of average percentage BOLD signal changes in response to nociceptive heat stimulation within parasylvian areas across animals. A–C, E–F. Plots of average % BOLD signal changes derived from contralateral (black lines) and corresponding ipsilateral (red lines) regions. Time courses obtained from control regions are plotted as gray lines. Error bars indicate standard errors. The 24 sec stimulus duration period is shown by the pale orange background block in each plot. *: magnitude difference is significant at $p < 0.05$. **: magnitude difference is significant at $p < 0.001$. &: magnitude of undershoot difference is significant at $p < 0.01$. D. Comparison of BOLD signal changes among parasylvian areas: bilateral pIns (solid and dash red lines), S2/PV (solid and dash green lines), Ri (solid and dash blue lines), and contralateral Ins (orange line). X-axis: time in image volume, one volume = 1.5 sec. Light orange background blocks indicate the stimulus duration of 24 sec.

NIH-PA Author Manuscript
NIH-PA Author Manuscript
NIH-PA Author Manuscript

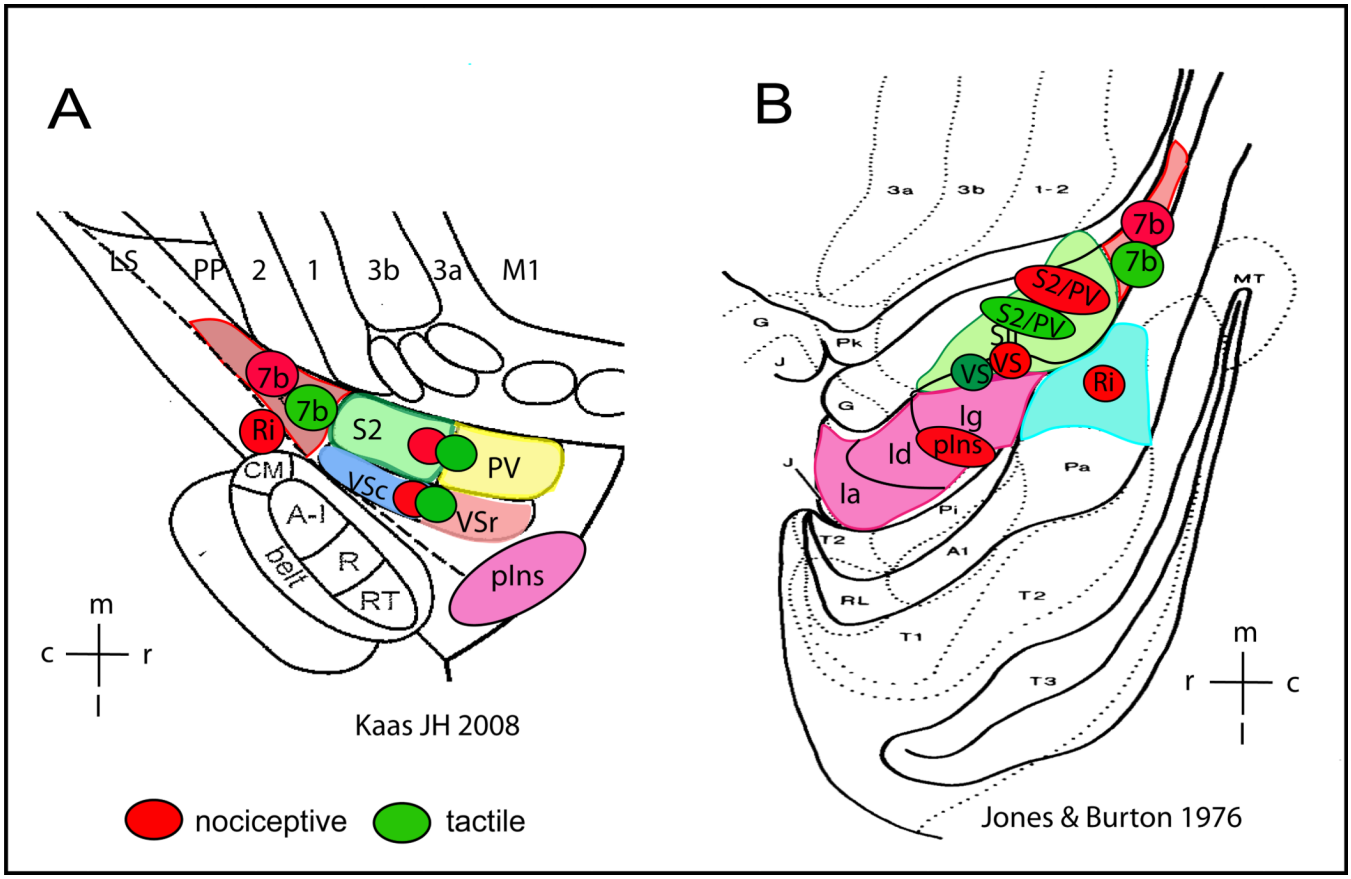

Figure 6.

Schematic summary of cortical areas that are responsive to nociceptive heat (red patches) and tactile (green patches) stimuli in anesthetized squirrel monkeys. Responsive cortical areas are indicated by color circles and placed over the schematic illustrations of cortical areas near the lateral sulcus in New World monkeys as established by two research groups (adapted from Kaas JH 2008 (A) and Jones & Burton 1976(B)). A: electrophysiologically and cytoarchitectonically defined cortical areas in New World monkeys. Ri: retroinsula; insula; Ins: insula; S2: secondary somatosensory area; PV: parietal ventral area; VSr: rostral ventral somatosensory area; VSc: caudal ventral somatosensory area; 7b: area 7b. m: medial; l: lateral; c: caudal; r: rostral. B: Cytoarchitectonically defined cortical areas in squirrel monkeys. SII includes subregions of S2, PV, VSc, VSr in Kaas 2008 (A). Insular cortex is divided into three subregions: Ig (granular field), Id (dysgranular field), and Ia (agranular field). Ri is located posterior to Insular region.

High-resolution fMRI revealed distinct and shared nociceptive heat and innocuous tactile processing networks within posterior parasylvian region of monkeys

NIH-PA Author Manuscript
NIH-PA Author Manuscript
NIH-PA Author Manuscript

Table 1

Frequency of activation in each area

		S2/PV	VS	area 7b	pIns	Ri
Nociceptive	Contralateral	10/12	10/12	7/12	7/12	8/12
		83%	**83%**	**58%**	**58%**	**67%**
	Ipsilateral	8/12	8/12	6/12	7/12	7/12
		67%	**67%**	**50%**	**58%**	**58%**
Tactile	Contralateral	6/9	3/9	4/9	2/9	4/9
		67%	33%	44%	22%	44%
	Ipsilateral	7/9	5/9	3/9	3/9	5/9
		78%	**56%**	33%	33%	**56%**

NIH-PA Author Manuscript
NIH-PA Author Manuscript
NIH-PA Author Manuscript

Table 2

Two gama fitting parametes and statistical significance

Fitting Parameter					Statistical Significance (p value)		
Area	**Peak (%)**	**TTP (s)**	**UShot(%)**	**R**	**Peak**	**TTP**	**Ushot**
Contra_S2/PV	0.33	18.9	−0.10	0.99	0.186	0.366	0.009 *
Ipsi_S2/PV	0.37	17.4	−0.21	0.99			
Contra_Ri	0.37	14.4	−0.15	0.99	5.00E-4 *	0.126	0.363
Ipsi_Ri	0.50	17.2	−0.21	0.98			
Contra_VS	0.61	18.6	−0.23	0.99	5.00E-4 *	0.442	0.185
Ipsi_VS	0.37	17.3	−0.09	0.98			
Contra_pIns	0.53	17.7	−0.11	0.99	5.00E-4*	0.803	0.410
Ipsi_pIns	0.32	17.2	−0.14	0.98			
Contra_7b	0.35	18.6	−0.13	0.99	0.616	0.331	0.009*
Ipsi_7b	0.34	16.2	−0.23	0.99			

*Statistically significant